

Above-Threshold Ionization As a Probe of Multielectron Physics

L. D. Van Woerkom¹, M. J. Nandor¹, M. A. Walker¹, G. D. Gillen¹, and H. G. Muller²

¹*Department of Physics, Ohio State University, 174 W. 18th Avenue, Columbus, Ohio, 43210-1106 USA*

²*FOM Instituut voor Atoom-en Molekulfysica, Amsterdam, 1098 SJ Netherlands*

Abstract—The study of above-threshold ionization (ATI) is now over 20 years old and much has been learned about the interaction of a single atomic electron with intense laser fields. The development of stable, high repetition rate ultrashort pulse laser systems has allowed experiments to probe intricate details of the ionization process using photoelectron and photoion spectroscopies. To date the overwhelming majority of data show that intense laser fields interact with only a single electron at a time to produce the well known features in electron kinetic energy spectra. We will present an overview of state-of-the-art experiments in ATI and show what can be learned about multielectron effects using careful measurements. Argon data showing the dominance of single electron physics at laser intensities near and below 10^{14} W/cm² will be shown. In addition, new data taken with a model two-electron system (magnesium) continues the search for detailed a understanding of intense field interactions in complex atoms. In all cases the current status of what we learn using ATI will be shown and discussed.

1. INTRODUCTION

When an isolated atom or molecule encounters an intense laser pulse, the probability that it will simultaneously absorb several laser photons becomes nonnegligible. Several processes which were previously inaccessible become probable ranging from atomic excitation, to ionization, to highly nonlinear upconversion of the incident light frequency. The study of these processes has now been going on for over two decades, and owes its origin to the development of laser sources capable of producing the necessary intensity for their observation. Since the beginning, breakthroughs in the technology of ultrashort laser pulses have been accompanied by breakthroughs in the study of the interactions of these pulses with atoms. Today there is a considerable amount of accumulated knowledge and understanding of the phenomena involved in the absorption of many photons.

There are several reviews [1, 2] in the literature for those unfamiliar with the development of this field. Here we intend to focus on the recent interest of researchers in multielectron effects or lack thereof, as relevant to observations of total ionization yields, electron kinetic energies and angular distributions of the ejected photoelectrons. First we will briefly highlight some of the major developments in the study of above-threshold- ionization (ATI) and what made them possible. We will then describe some results of our own investigations into possible multielectron signatures in the ATI

spectra of argon. Finally, we will present preliminary experimental results of studies in magnesium for a variety of laser intensities and photon energies.

2. BACKGROUND

Figure 1 shows a brief timeline of important milestones in the areas of high intensity photoionization and above-threshold ionization (ATI). Once an atom encounters a laser of sufficient intensity that it can absorb enough photons to ionize, it seldom stops there, choosing instead to absorb a few or often many more than the minimum number necessary to ionize. This process is called ATI and was first observed by Agostini et al. in 1979 [3]. Today, it is commonplace to observe ATI by recording the kinetic energy distribution of the photoelectrons it produces using time-of-flight spectroscopy. As technology has developed more sophisticated laser sources and detection techniques, experimental ATI spectra have in turn become more and more detailed, and the effort required for a complete understanding of their features has grown considerably.

The first ATI spectra observed consisted of a series of structureless peaks separated by the photon energy with decreasing amplitude, consistent with a perturbative interpretation indicating that absorbing more photons should be less likely. As accessible intensities increased and pulsewidths decreased, effects such as channel closure [4] and Freeman resonances [5] were seen to suppress the low order peaks and to cause subpeak structure in “short” pulse spectra. These pointed out the importance of changes in the atomic structure caused by the field (ac Stark shifts), and to the equally important role of the dynamics of free or nearly free electrons in the intense ac field. An important concept for understanding both of these is the ponderomotive (wiggle) energy U_p imparted to loosely bound and ionized electrons by the laser.

The next important step in the development came when short pulse lasers capable of operating at kilohertz repetition rates became available. These increased the available dynamic range of ATI experiments by orders of magnitude. With increased sensitivity came the discovery that electrons escaping from the ion core could in fact be accelerated back into it by the field, whereupon they are able to acquire additional kinetic energy [6, 7]. These electrons produce a “plateau” in the ATI spectrum, with a characteristic cutoff energy which often extends up to dozens of photons above the ionization limit, and which in some cases can account for a significant fraction of the total electron yield. Again many of the characteristics of this plateau could be explained by extending the semiclassical “simpleman’s” model to include an elastic rescattering event [6, 8]. However, as expected of such a simplified model, there remained effects for which it could not provide an explanation. More sophisticated theories

existed, but the difficulty of calculating a complete ATI spectrum to high order with high energy and intensity resolution was prohibitive. This was not seen to be a problem at the time, since it was felt that the essential physics had been extracted from the available data.

In 1997, however, two groups reported observations of narrow energy structures in the plateaus of argon [9] and xenon [10], whose amplitudes were strongly intensity dependent, but whose energy positions were not. In Fig. 2, these data are shown as a series of spectra taken at increasing laser intensities, in which groups of peaks in specific energy intervals were observed to appear and dominate at certain points. The behavior of these peaks suggested that they were due to a resonant process of some kind. The fact that the peaks have energy positions which reach high into the single electron continuum was cause for speculation that multiply excited states could be involved in the enhancement of their relative strengths in the spectra. Several possibilities existed to explain the phenomena; among these were that they were manifestations of (1) interferences between rescattered single-electron wavepackets, (2) excitations of core excited states caused by the coupling of the laser to the core via correlated wiggles, which then decayed via laser-assisted Auger [11], (3) multiple excitation via a shake-off mechanism similar to that seen for single UV photon ionization, and (4) independent (uncorrelated) excitations of two electrons via a multiphoton isolated core excitation scenario.

The central question was whether the existing single electron theory could account for the data. Perhaps its best implementation had been in direct numerical integration of the Schrödinger equation in the space representation for a single electron bound by a static core potential [12], the so-called “single active electron” (SAE) approximation. Other single electron methods existed as well [2, 12] and had been important and successful for understanding elements of the physics, but none of the existing avenues had been pursued to the point of actually calculating a spectrum, for the reasons mentioned previously.

A single electron code was developed in 1997 by H.G. Muller [13] for the purpose of calculating an ATI spectrum with enough resolution at high energy to attempt to reproduce the features seen in argon by Hertlein *et al.* [9]; specifically, it was hoped that the results would reveal differences that could be traced to multielectron effects. Instead the calculation seemed to qualitatively reproduce the effects. A collaboration with Muller resulted in a careful comparison of experiment and theory over a wide range of kinetic energies and laser intensities.

The theoretical portion of the comparison was performed by running the Muller code for several hundred individual laser intensities. Since the output consisted essentially of the response of the atom to a single laser intensity, it was necessary to perform a spatially and temporally weighted sum of results

from several individual intensities to generate a spectrum which could be compared to the experiment [14].

The details of the experiment are described elsewhere [14], but to summarize briefly, argon spectra were taken using a restricted volume technique, with the laser power controlled via attenuation by a half wave plate and polarizer. Spectra were collected for 35 different laser powers with high time resolution (<40 ps). The intensities were calibrated to within 8% and the energy resolution was better than 40 meV over the entire spectrum (up to 50 eV).

Figure 3 shows a comparison of data and calculation spanning a large kinetic energy range. The broad features of the experimental envelope as well as the detailed structure of individual ATI orders are largely reproduced by the calculation. Figure 4 illustrates the agreement for low kinetic energies and a variety of peak laser intensities. The appearance intensities of individual resonant contributions match, again validating the essence of the simple model of ponderomotively shifted Freeman resonances.

4. ATI AND ION YIELDS IN MAGNESIUM

The results for argon clearly illustrate that the majority of the physics is well described by single electron physics. In order to more directly search for the manifestation of multielectron effects, magnesium was chosen as a model two-electron system.

The laser system used in this investigation was a tunable regeneratively amplified Ti:Sapphire laser with 120 fs pulse duration and a 1 kHz repetition rate similar to that used for the argon experiments. For all of the ionic yield experiments the system was tuned to 800 nm. The central wavelength was tuned as far as 840 nm for some photoelectron data while maintaining the same pulsewidth. The laser intensity in the interaction region was calibrated by collecting photoelectron spectra of argon for a variety of pulse energies. These spectra were then compared to spectra taken in the previous investigation [14] using the appearance of the 8-photon Freeman resonance of the 4-f Rydberg level as a calibration point.

The laser was focused into the vacuum chamber and propagated into the interaction region mutually orthogonal to the atomic beam and the ion/electron flight path. For linear polarization ion yields and all of the photoelectron spectra, the polarization was oriented parallel to the flight path. When circular polarization was desired, a quarter wave plate was placed in the beam path and optimized for proper angular alignment. To reduce the effects of spatial averaging a restricted volume technique [8] was employed by placing a pinhole in the flight path near the interaction region. The

atomic beam was generated by a low-temperature (0 to 1000°C) effusion cell with the beam terminated on a cold plate attached to a large capacity (15 liter) liquid nitrogen trap.

The ions were extracted from the interaction region by a static electric field. The measured ionic yield curves are displayed in Fig. 5 for linear polarization, and Fig. 6 for circular polarization. Each point is an integration of all of the counts detected for the three isotopes of each ionic species from each mass spectrum, and normalized to one million laser shots per data point, although up to 10 million shots were taken for a given data run.

For both figures some overall structure is evident. The first ionic species yield increases near linearly on the log-log plot until the saturation intensity is reached and then flattens out. For a restricted volume experiment, the volume of an incremental intensity range below the maximum intensity does not continue to grow as the energy per pulse is increased. For the second ion a two-rate process is evident. The first rate initially increases and then slows down. Then at $6 \times 10^{13} \text{ W/cm}^2$ the yield starts to increase again for both polarizations. At the highest intensity of $1.2 \times 10^{14} \text{ W/cm}^2$ the second ion yield curve is beginning to saturate for both polarizations. The most prominent gross structural difference between the linear and circularly polarized light is the overall yield of double ions. The yield of double ions is dramatically suppressed when the polarization is changed from linear to circular. At the saturation limit, the yields differ only by a factor of 2. In the region below saturation, the yield of the linear polarization curve ranges from 2 to 3 orders of magnitude higher than that for circularly polarized light.

The photoelectron spectra (PES) in this study were an investigation of the above threshold ionization (ATI) structure for magnesium with a variety of intensities and wavelengths for 120 fs pulses. Since this was a preliminary investigation, a full volume interaction region was used to increase the count rate and detection efficiencies. Figure 7 shows an energy level diagram for magnesium. The gray lines are separated by 1.55 eV intervals representing 800 nm photons. Figure 8 is the same diagram, but with photon spacing of 1.476 eV, corresponding to a wavelength of 840 nm. The table shows the photon order processes for direct and sequential ionization channels with 800 nm laser light.

When the laser was tuned from 800 nm to 840 nm 3 parity-allowed transitions were tuned into or near resonance and a channel closing occurred as illustrated in Fig. 7. (i) The energy of a 3-photon absorption comes into near resonance with a non-pondermotively shifted $3s3p \text{ } ^1P$ state. (ii) The energy of a 5-photon absorption falls below the first ionization limit and into a densely populated energy region of high lying Rydberg states. (iii) The energy of a 7-photon absorption comes into near resonance with the

3p3d 1F autoionizing state. (iv) The energy of an 8-photon absorption shifts into a densely populated series of autoionizing 3pNp 1S Rydberg states.

Figure 9 is a collection of PES for the same intensity, $9 \times 10^{13} \text{ W/cm}^2$, and different laser wavelengths. The laser was tuned from an initial 800 nm out to 840 nm while maintaining the same energy per pulse and pulsewidth. The PES of the 800, 810, and 820 nm wavelengths all have about the same peak counts for each ATI order. The entire spectrum for the 810 and 820 nm data were each suppressed to eliminate complete overlap of each other on the graph and allow for easier comparison. When the laser was tuned to 840 nm the PES spectrum changed so dramatically that it is displayed separately above, but to the same energy scale. Figure 10 is a collection of PES for different intensities and a wavelength of 800 nm. The energy axis is expanded to show a more detailed spectrum of the first two ATI orders. For each ATI order the converging series of Rydberg f-states is displayed. The vertical lines located at 2.24, 2.55 eV, etc. corresponds to two photon energies above the 3s4f, 3s5f, etc. states. The lines at 3.1 and 4.65 eV correspond to 2 and 3 photons energies above the ionization limit.

As mentioned previously, when tuning the wavelength from 800 to 840 nm, several processes were encountered. The first process of bringing a three-photon energy to just above the 3s3p 1P allows this state to become populated early in the pulse. This three-photon process is likely to occur for lower intensities that are present early in the pulse. These lower intensities will occur before the state is pondermotively shifted out of resonance and the channel is closed. The photoionization process and transition possibilities can then change dramatically if this population is subjected to the majority of the laser pulse.

The second process closes the five-photon ionization channel for most of the Rydberg states of the neutral atom. This is clearly evident in Figs. 9 and 10. For an intensity of $9 \times 10^{13} \text{ W/cm}^2$ each ATI order consists of a high peak at the 4f resonance, and a shoulder to higher energy for the fifth, sixth, and higher Rydberg states. As the wavelength is tuned from 800 to 820 nm this shoulder disappears. The effect is more noticeable in the third and fourth ATI orders around 5 and 7 eV. As the 5-photon energy drops below the ionization limit the ionization channels close for the high Rydberg states, and those just below this energy level as they will be pondermotively shifted out of resonance. These channel closings will eliminate the high-energy shoulder in the ATI spectrum.

The effects of the third and fourth processes of tuning the 7-photon energy towards the 3p3d autoionizing state and the 8 photon energy into the 3pNp autoionizing Rydberg series are not as easily identifiable and warrant further investigation.

5. CONCLUSIONS

The use of above-threshold ionization as a probe of high field atomic physics continues to yield new information. The interaction of argon and laser light up to about 1×10^{14} W/cm² can be explained using single electron physics. Furthermore, we have measured ionization yields of singly and doubly charged magnesium ions for the intensity range of 8×10^{12} to 2×10^{14} W/cm² for both linearly and circularly polarized light and photoelectron spectra at an intensity of 9.4×10^{13} W/cm² for laser wavelengths between 800 and 840 nm. The ionic yield results show a single-rate process for the first ion, and a two-rate process for the double ion for both polarizations. The enhancement of the double ion occurs in an intensity region below the saturation of the first ion revealing a nonsequential process. When the laser wavelength is tuned from 800 to 840 nm a channel closing for the 5-photon ionization of the higher Rydberg states occurs eliminating the high energy shoulder in each ATI order and then the photoelectron spectrum changes dramatically as several autoionizing states are brought into resonance or near resonance.

REFERENCES

1. DiMauro, L.F. and Agostini, P., 1995, *Adv. At. Mol. Opt. Phys.*, **35**, 79.
2. Joachain, C.J., Dörr, M., and Kylstra, N., 2000, *Adv. At. Mol. Opt. Phys.*, **42**, 225.
3. Agostini, P., Fabre, F., Mainfray, G., *et al.*, 1979, *Phys. Rev. Lett.*, **42**, 1127.
4. Petite, G., Agostini, P., and Muller, H.G., 1988, *J. Phys B*, **21**, 4097.
5. Freeman, R.R., Bucksbaum, P.H., Milchberg, H., *et al.*, 1987, *Phys. Rev. Lett.*, **59**, 1092.
6. Schafer, K.J., Yang, B., DiMauro, L.F., and Kulander, K.C., 1993, *Phys. Rev. Lett.*, **70**, 1599.
7. Paulus, G.G., Nicklich, W., Huale, X., *et al.*, 1994, *J. Phys. B*, **27**, L1.
8. Corkum, P., 1993, *Phys. Rev. Lett.*, **71**, 1994.
9. Hertlein, M.P., Bucksbaum, P.H., and Muller, H.G., 1997, *J. Phys. B*, **30**, L197.
10. Hansch, P., Walker, M.A., and Van Woerkom, L.D., 1997, *Phys. Rev. A*, **55**, R2535.
11. Bucksbaum, P.H., Sanpera, A., and Lewenstein, M., 1997, *J. Phys. B*, **30**, L843.
12. Kulander, K.C., Schafer, K.J., and Krause, J.L., 1992, *Atoms in Intense Laser Fields* (Boston: Academic).
13. Muller, H.G., 1999, *Laser Phys.*, **9**, 138.
14. Nandor, M.J., Walker, M.A., and Van Woerkom, L.D., 1999, *Phys. Rev. A*, **60**, R1771.

FIGURES

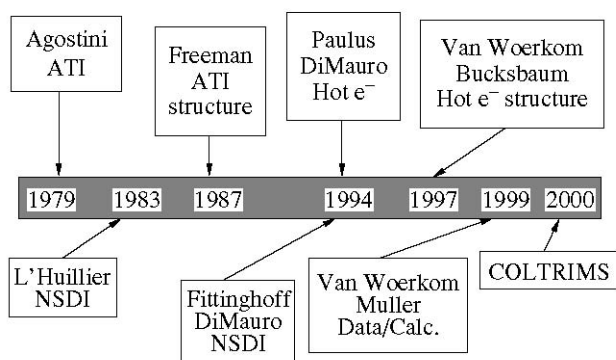


Fig. 1. ATI timeline.

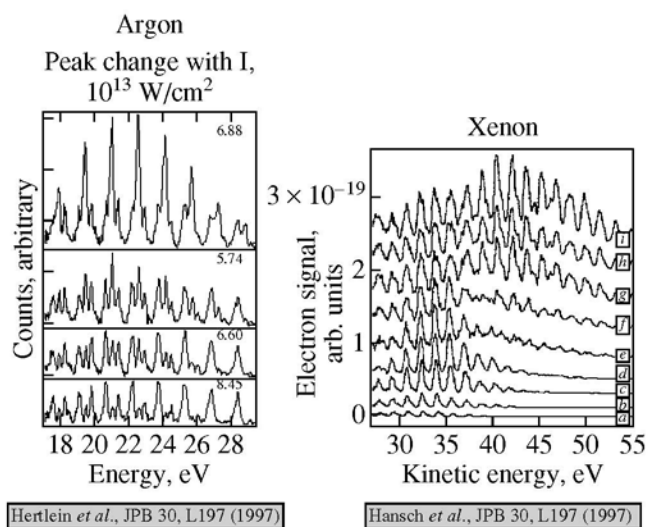


Fig. 2. Appearance of resonant structure in the hot-electron spectrum.

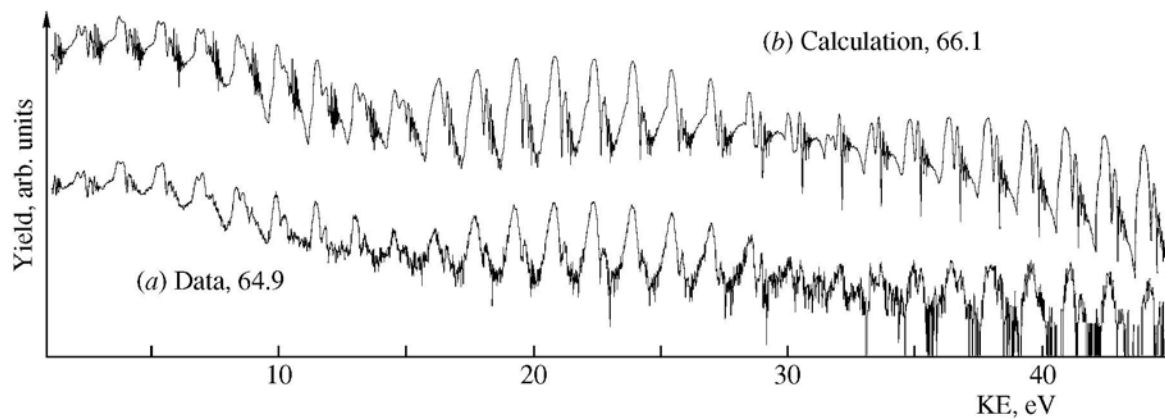


Fig. 3. Comparison of argon data and single electron calculation.

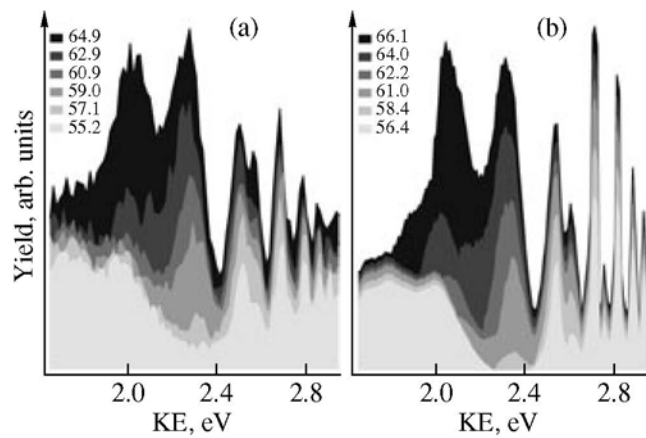


Fig. 4. Detailed comparison of argon data and single electron calculation.

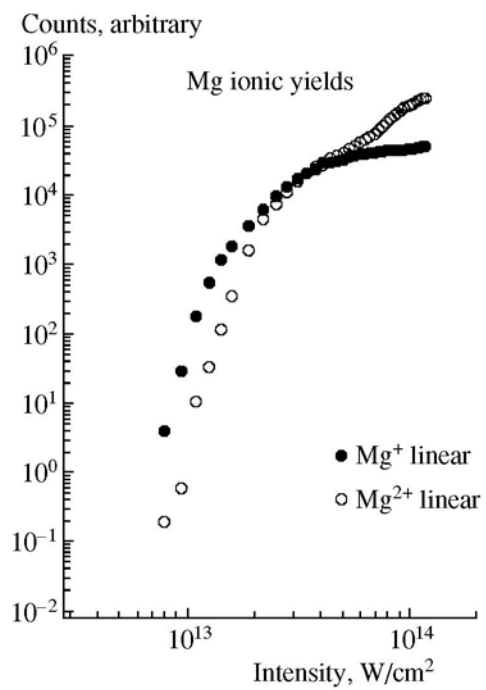


Fig. 5. Magnesium ionic yields for linearly polarized light.

Table. Sequential and direct ionization processes

$\text{Mg}(3s^2) + 5\gamma \longrightarrow \text{Mg}^+(3s) + e^-$
$\text{Mg}^+(3s) + 10\gamma \longrightarrow \text{Mg}^{2+} + e^-$
$\text{Mg}(3s^2) + 15\gamma \longrightarrow \text{Mg}^{2+} + 2e^-$

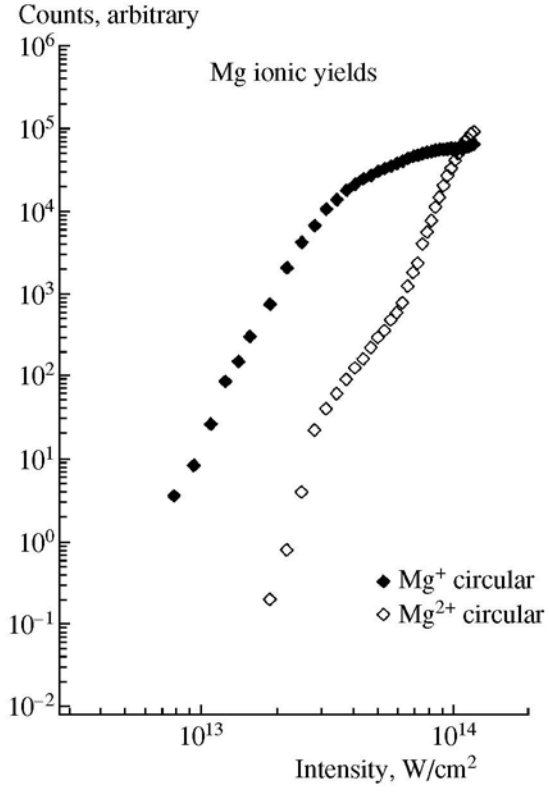


Fig. 6. Magnesium ionic yields for circularly polarized light.

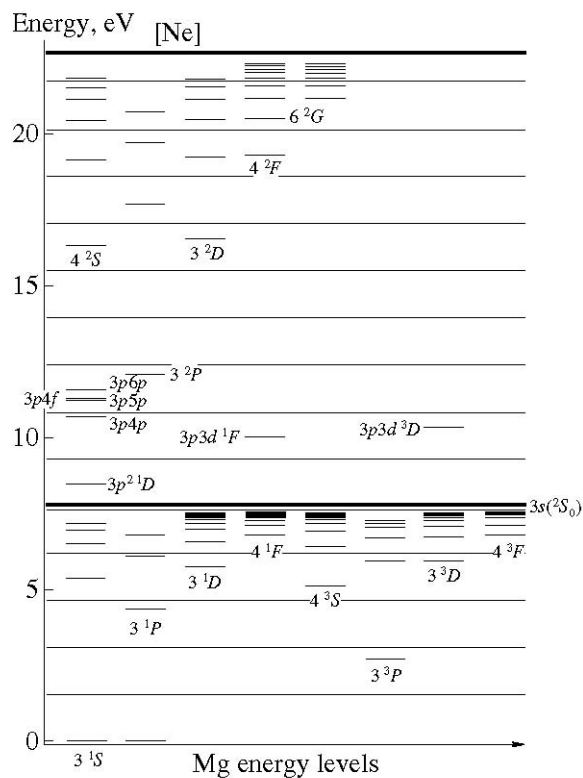


Fig. 7. Energy level diagram for magnesium and 800 nm photons (gray lines are spaced every photon energy at 1.55 eV).

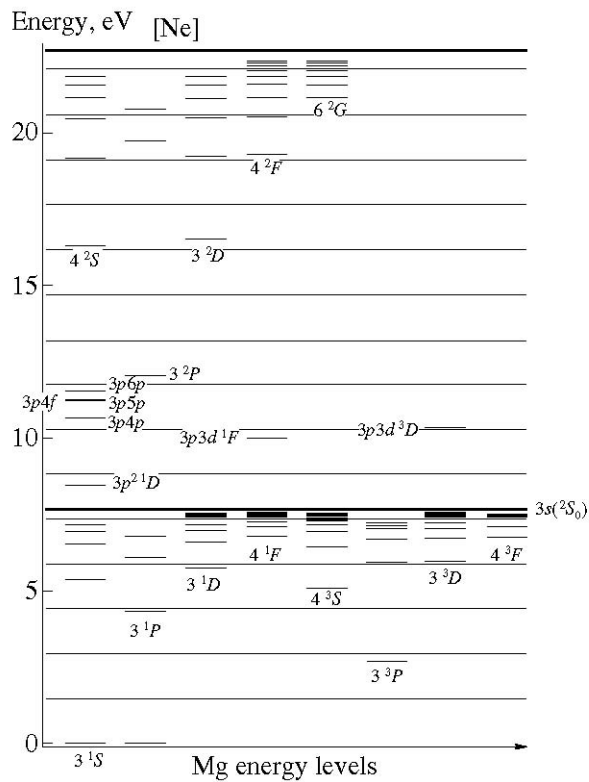


Fig. 8. Energy level diagram for 840 nm photons (gray lines are spaced every photon energy at 1.48 eV).

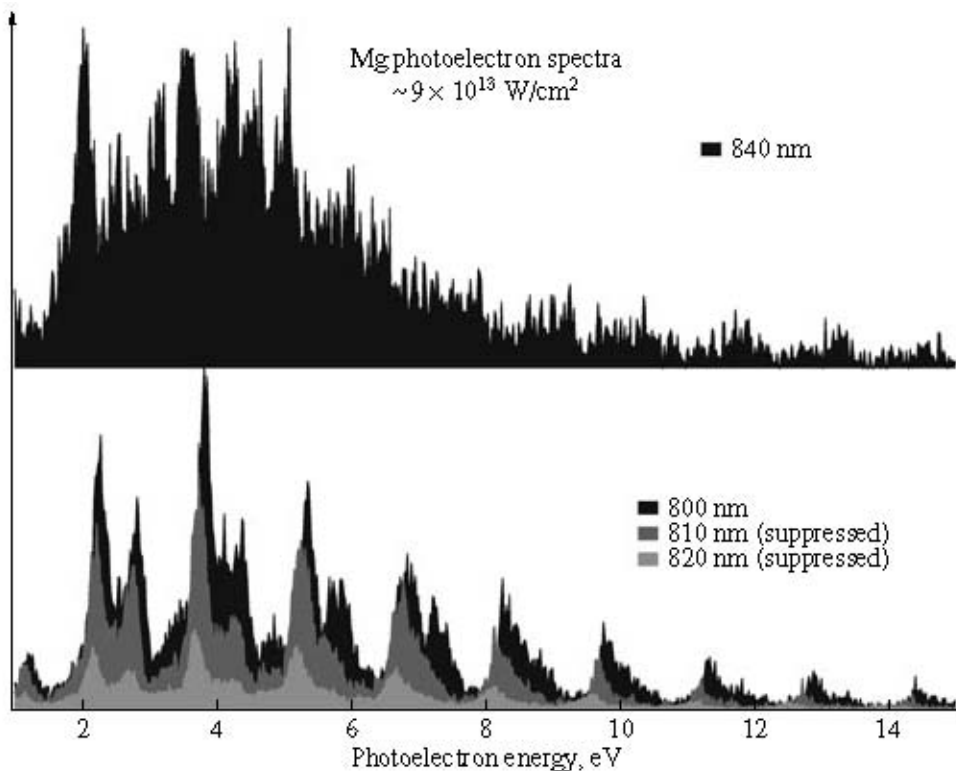


Fig. 9. PES for different wavelengths. The spectra at 810 and 820 nm have been suppressed for easier comparison.

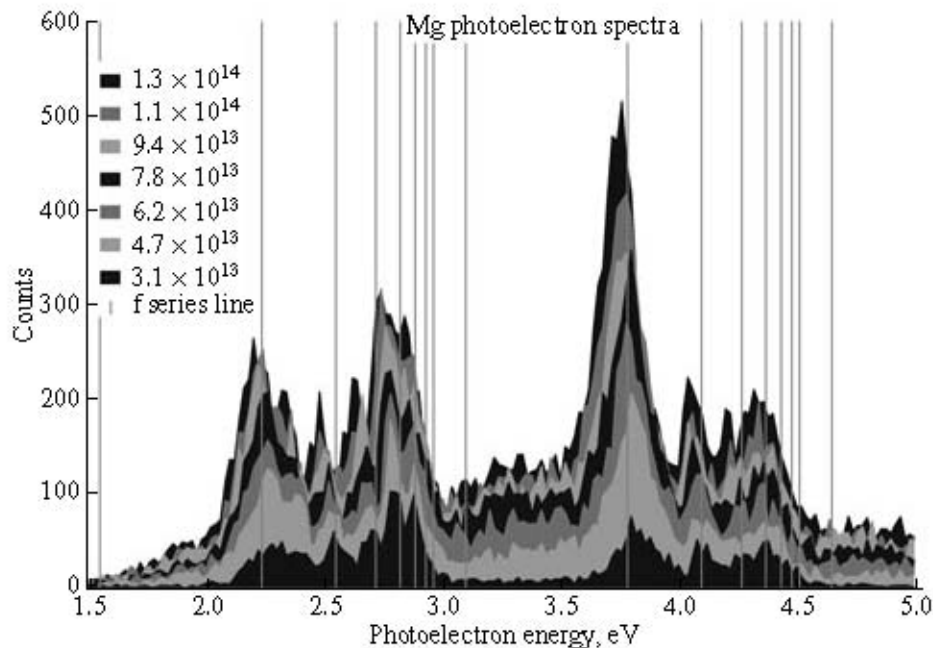


Fig. 10. Low kinetic energy electron spectra for various intensities at 800 nm.